



HAL
open science

A variety of radars designed to explore the hidden structures and properties of the Solar System's planets and bodies

Valérie Ciarletti

► **To cite this version:**

Valérie Ciarletti. A variety of radars designed to explore the hidden structures and properties of the Solar System's planets and bodies. *Comptes Rendus. Physique*, 2016, 17 (9), pp.966-975. 10.1016/j.crhy.2016.07.022 . insu-01368065

HAL Id: insu-01368065

<https://insu.hal.science/insu-01368065>

Submitted on 20 Sep 2016

HAL is a multi-disciplinary open access archive for the deposit and dissemination of scientific research documents, whether they are published or not. The documents may come from teaching and research institutions in France or abroad, or from public or private research centers.

L'archive ouverte pluridisciplinaire **HAL**, est destinée au dépôt et à la diffusion de documents scientifiques de niveau recherche, publiés ou non, émanant des établissements d'enseignement et de recherche français ou étrangers, des laboratoires publics ou privés.



Distributed under a Creative Commons Attribution - NonCommercial - NoDerivatives 4.0 International License



ELSEVIER

Contents lists available at ScienceDirect

Comptes Rendus Physique

www.sciencedirect.com



Probing matter with electromagnetic waves / Sonder la matière par les ondes électromagnétiques

A variety of radars designed to explore the hidden structures and properties of the Solar System's planets and bodies

Une diversité de radars conçus pour révéler et caractériser les structures cachées des petits corps et planètes du système solaire

Valérie Ciarletti

LATMOS/IPSL, UVSQ Université Paris-Saclay, UPMC Université Paris-6, CNRS, 78280 Guyancourt, France

ARTICLE INFO

Article history:

Available online xxxx

Keywords:

Radar
Space missions
Electromagnetic wave propagation

Mots-clés :

Radar
Missions spatiales
Propagation des ondes électromagnétiques

ABSTRACT

Since the very first observations of the Moon from the Earth with radar in 1946, radars are more and more frequently selected to be part of the payload of exploration missions in the Solar System. They are, in fact, able to collect information on the surface structure of bodies or planets hidden by opaque atmospheres, to probe the planet subsurface or even to reveal the internal structure of a small body comet nucleus.

A brief review of radars designed for the Solar System planets and bodies' exploration is presented in the paper. This review does not aim at being exhaustive but will focus on the major results obtained. The variety of radars that have been or are currently designed in terms of frequency or operational modes will be highlighted.

© 2016 Académie des sciences. Published by Elsevier Masson SAS. This is an open access article under the CC BY-NC-ND license

(<http://creativecommons.org/licenses/by-nc-nd/4.0/>).

R É S U M É

Depuis les premières observations radar de la Lune depuis la Terre en 1946, les radars font de plus en plus fréquemment partie de la charge utile des missions d'exploration du système solaire. Ils sont, en effet, capables de recueillir des informations à la fois sur la structure superficielle d'un corps ou d'une planète à travers une atmosphère optiquement opaque, de sonder le sous-sol d'une planète, ou encore de révéler la structure interne d'un petit corps.

Une revue non exhaustive des radars scientifiques développés pour l'exploration des planètes et autres corps du système solaire est présentée dans cet article. Quelques résultats majeurs sont présentés. L'accent est mis sur la variété des radars qui ont été et sont actuellement conçus en terme de fréquence ou de mode opératoire en fonction des contraintes de la mission et des objectifs visés.

© 2016 Académie des sciences. Published by Elsevier Masson SAS. This is an open access article under the CC BY-NC-ND license

(<http://creativecommons.org/licenses/by-nc-nd/4.0/>).

E-mail address: Valerie.Ciarletti@latmos.ipsl.fr.

<http://dx.doi.org/10.1016/j.crhy.2016.07.022>

1631-0705/© 2016 Académie des sciences. Published by Elsevier Masson SAS. This is an open access article under the CC BY-NC-ND license (<http://creativecommons.org/licenses/by-nc-nd/4.0/>).

Please cite this article in press as: V. Ciarletti, A variety of radars designed to explore the hidden structures and properties of the Solar System's planets and bodies, C. R. Physique (2016), <http://dx.doi.org/10.1016/j.crhy.2016.07.022>

1. Introduction

Radars have a unique capacity to provide remote information about targets that cannot be reached by other kinds of instruments. In planetary science, they have been successfully used to reveal the topography of the surface of a solar system's bodies hidden by thick atmospheres (such as impact craters and volcanoes on Venus, lakes and possible cryovolcanoes on Titan), the structures and layers buried under the surface of planets giving thus access to their geological history (internal layering of the polar caps of Mars, thickness of lava flows on the Moon) or even the internal structure of small bodies (Churyumov–Gerasimenko).

The basic principle of radars is simple: it is based on the transmission and eventually reception of an electromagnetic wave that has propagated through and interacted with the sounded environment. After more or less complicated signal processing, the radar determines for each detected echo a propagation delay and its associated amplitude. Both quantities are then processed to retrieve information on the geometrical and dielectric properties of the target and of the propagation environment between the target and the antennas. The instrument's final radiometric performances depend on the radar's parameters, on the geometrical configuration, on the sounded environment properties and on the optimal use made on the redundancy within the measurements.

Section 2 of this paper presents the main kinds of radars that have been designed to explore the Solar System's bodies and planets. The emphasis is put on the platforms those radars can be accommodated on (i.e. spacecraft in orbit or flyby, rover mobile at the surface, and even stationary lander on the surface), and on the choice of a center frequency according to the scientific and technical objectives to reach.

An overview of the main radar experiments designed for planetary exploration and some of the most significant results they obtained are presented in the second section.

2. Radars for planetary exploration and science

Radars were originally developed for military purposes, which has rapidly contributed to the development of a number of civil applications for safe travel and remote sensing of the Earth environment. For decades now, the famous radar equation has been the basis to design radars [1], especially for planetary exploration where distances to the targets are often extremely large and where very little information is available on the target's characteristics.

2.1. Choosing the platform

The first historic observations of the Moon were made from the Earth in 1946 at 138 MHz by the Corps' Evans Signal Laboratory, New Jersey [2,3]. After some unsuccessful attempts, in 1961, Venus became the first planet of the Solar System to be explored by a radar from the Earth: the 34-m dish of the Goldstone Observatory in California [4,5] was used at first, followed later by the 300-m diameter antenna at Arecibo [6].

Since the 1980s, the vast majority of radars used in planetary science have been operated on missions that offered the opportunity to map a whole planet from orbit (the MarsExpress [7] and Mars Reconnaissance Orbiter [8] missions around Mars, the Magellan mission to Mercury [9]) or during a number of limited flybys (the Cassini mission to Saturn and its moons [10]). In addition, radars dedicated to a more accurate but local subsurface characterizations can be accommodated on board vehicles mobile at the surface of planets. The recent Chang'e-3 mission [11] landed on the Moon a rover equipped with a Ground Penetrating Radar (GPR) in order to sound the lunar regolith from the surface. The next ESA and NASA rover missions to Mars, ExoMars [12] and Mars2020 will also operate GPRs to sound the Martian subsurface along the rover's paths.

Less conventional experiments have been specifically designed to retrieve information on the subsurface structure and its dielectric properties in very specific contexts. Among those, we can mention two bi-static radars:

- the CONSERT experiment of the *Rosetta* mission, designed to perform the tomography of comet 67P/Churyumov–Gerasimenko nucleus, is composed of two separated units, the first one being located on the surface of the nucleus while the other one is on-board the orbiter [13];
- the EISS (Electromagnetic Investigation of the Sub-Surface) bistatic radar was selected on the now canceled Humboldt payload of the ExoMars mission. The instrument is able to take advantage of the simultaneous presence of a stationary lander and a mobile rover to perform deep sounding of the Martian subsurface around the landing site. In monostatic mode, the 35-m-long electrical antennas located on the stationary platform of the mission are used for transmission and reception. While in bistatic mode, a 10-cm-long magnetic receiver accommodated on the mission's rover is able to measure three orthogonal components of the magnetic field too. These measurements allow one to retrieve the direction of arrival of each reflected wave and thus to retrieve the 3D location of the buried reflectors for a better understanding of the geological context of the site [14–16].

Finally, on a number of space missions, opportunity bi-static experiments (often referred to as radio science experiments) take advantage of existing communication channels of the spacecraft with Earth to perform limited soundings of the planet's

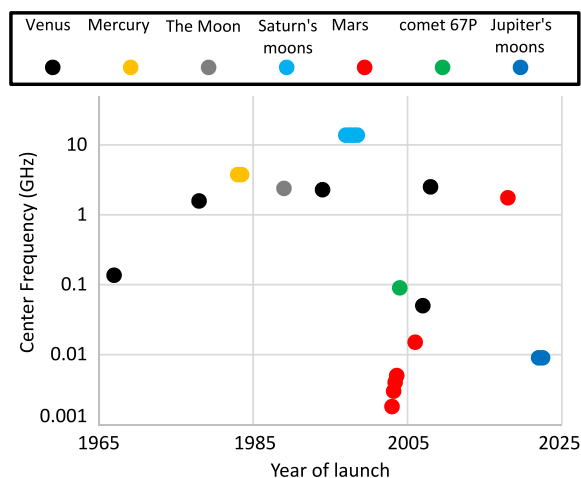


Fig. 1. Center frequency of the main radars that have been designed for planetary exploration. For each instrument, the target is indicated by the color code.

subsurface at grazing incidence angles (for example, the **Mars Radio Science** experiment [17] on-board the MarsExpress spacecraft, the Clementine bi-static radar experiment at the Moon [18], and the Viking bistatic radar on Mars [19]).

2.2. Designing the right radar

The specifications for each instrument of a mission payload are based on the scientific objectives of the mission. For a radar, the characteristics of the target (range, geoelectrical and geometrical properties) as well as the final product (image, topography, estimated roughness and dielectric properties, subsurface characterization) and resolution aimed at will guide the radar design.

2.2.1. A variety of operating modes

Most of the time, given the limited resources (of mass, volume and power) available in space missions, radars designed and developed for planetary missions are adaptable enough so that they can be operated in different modes making the best way of the hardware. They very often can be used as altimeters, synthetic-aperture radars, subsurface sounders, scatterometers and radiometers, and often also used to characterize the atmosphere and ionosphere when relevant.

A radar altimeter is usually a nadir-looking radar. It measures the power received after an interaction with the surface as a function of the propagation delay and thus provides an estimate of the distance between the radar and the reflecting surface. It is used to infer the topography of the surface. The radar altimeter echo profile is controlled by the range to the surface and the surface back-scattering properties, which depend on the surface roughness at scales larger than the wave length and on the dielectric properties of the shallow subsurface. High frequencies are usually chosen for radar altimeters, so as to limit penetration into the subsurface.

On the contrary, soundings radars are low-frequency HF Ground-Penetrating Radars. They are used to perform deep soundings (up to several hundreds of meters) of planetary sub-surface structures. The first radar sounder flown was ALSE (Apollo Lunar Sounder Experiment) [20] on board Apollo 17 in 1972. Two other sounders have explored the Martian sub-surface (§ 3.1.1): MARSIS (Mars Advanced Radar for SubSurface and Ionosphere Sounding) [21] on board the European Space Agency's Mars Express probe, and SHARAD (mars SHallow RADar sounder) [22] on the NASA Mars Reconnaissance Orbiter (MRO). A radar sounder has also been used on the Japanese Moon probe SELENE [23], launched in 2007 (§ 3.1.2).

A synthetic-aperture radar (SAR) is used to obtain images of an area at wavelengths that are significantly lower than those used by optical cameras. It uses the motion of the antenna over an area to improve the spatial resolution; therefore, SARs are typically mounted on moving spacecraft, but they might also be used on moving/rotating targets. Synthetic aperture radars are the most suitable instruments to provide images of planetary surfaces hidden by opaque atmospheres like Venus and Titan. The two Soviet spacecrafts Venera 15 and Venera 16 [24] provided images of the planet in 1983 using SAR and Radar altimeters. The SAR of the Magellan mission [25] later in 1990 achieved an almost complete coverage of the surface of Venus (§ 2.1.1). The SAR of the *Cassini* [26] spacecraft, in orbit around Saturn, has provided impressive images of Titan surface during flybys (§ 2.1.2). When possible, enhanced processing of SAR data allow us to provide the SAR-based topography of a surface with a much better resolution than the one obtained by simple radar altimeters.

2.2.2. A broad frequency range

The choice of the frequency is of the uppermost importance since it will drive the penetration depth. Moreover, because the bandwidth is limited by the central frequency, this choice will also set the range resolution (i.e. its ability to distinguish between two targets at different distances of the instrument). In the context of planetary missions, radars operating at

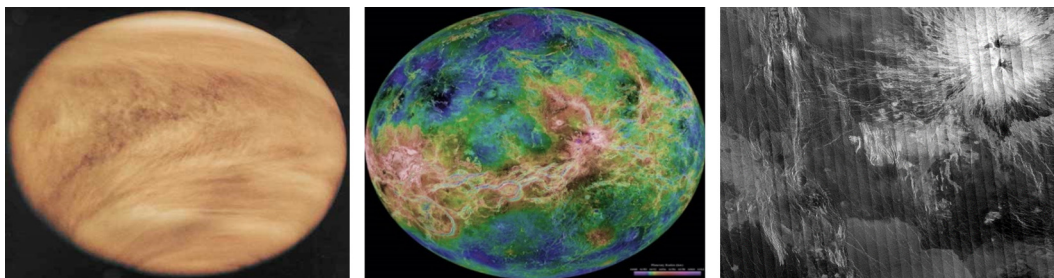


Fig. 2. Images of Venus Credit: NASA/JPL/USGS. Left: Ultraviolet image by the Pioneer Venus Orbiter spacecraft. This image reveals structures of the atmosphere that are not detected in the visible light image but the surface remains hidden [27]. Center: Topography of surface based on the Magellan radar's data with additional information from Venera and Pioneer Venus missions and Earth-based radar measurements. The lowest elevations are in blue (PIA00159). Right: image of a 1.5-km-high volcano with a resolution of ~ 675 m obtained by the Magellan SAR [33].

extremely different frequencies have been used (see Fig. 1). The largest wavelength has been used by the MARSIS sounder onboard the MarsExpress ESA mission: 230 m in the vacuum for a radar designed for kilometeric penetration depths to search for potential water reservoirs in the Martian subsurface. The shortest is 2.18 cm for the radar of the *Cassini* mission, whose primary objective is to characterize Titan's surface through its thick atmosphere.

As mentioned previously, the choice of the center frequency has an impact on the range resolution since the resolution improves when the bandwidth increases. As a consequence, radars designed to perform deep soundings of the subsurface must operate at low center frequencies and consequently have a poor vertical resolution. Comparison of the MARSIS and ShaRad sounders operated on Mars is a good illustration of the matter (Fig. 3). Another example of this trade-off is provided by the WISDOM radar of the future ExoMars mission's rover. It has been designed to provide high resolution images of the shallow Martian sub-surface in order to support drilling operations; as a consequence, it will operate on an especially large frequency bandwidth from 0.5 to 3 GHz, which will limit its penetration to a few meters.

In addition to these considerations, in the specific context of space missions, where the size and mass of the payload's instruments are always strongly limited, the choice of the frequency is also constrained by the size of the antenna used to transmit and receive the electromagnetic waves.

3. A variety of targets in the Solar System

The radar investigations of the Solar System started logically with Earth-based observations and aimed at the closest target to Earth, namely the Moon. Next came Venus and Mercury, followed by Mars and the moons of Saturn. Soon the moons of Jupiter will also be explored by radars. This section illustrates the impressive knowledge that has been acquired on the Solar System thanks to radar instruments.

3.1. Peering through a dense and opaque atmosphere

Radars have been successfully used to reveal the surface topography and geology of planetary bodies covered by thick and optically opaque atmospheres. Venus and Titan's exploration by radars provide the best illustrations of this capacity.

3.1.1. Venus

The surface of Venus is hidden by thick clouds of sulfuric acid that prevent optical remote sensing technics to access the surface [27] (see Fig. 2/right). Venera was a series of 16 flyby, orbital, and landed missions to Venus conducted by the Soviet Union from 1961 to 1983. Most of these missions failed because of the harsh Venusian environment. But since Venera 7, successful landings of modules able to survive for 30 to 120 min at the surface provided the first optical pictures of the Venusian ground.

The NASA Pioneer Venus Orbiter was launched in 1978 [28]. One of the main experiments on its payload was the radar (ORAD) operating at 1.757 GHz. This radar altimeter was used to get information on the surface topography which has been reconstructed with a vertical accuracy better than 200 m and a 150-km resolution. The surface electrical conductivity and roughness at 1-m scale have been estimated too. The Pioneer Venus Orbiter was the first spacecraft to use radar to obtain a global image of the Venus surface [29].

In 1983, the twin Venera 15 and 16 spacecrafts carried a radar altimeter and a SAR operating at 3.75 GHz that were used to map the topography of the surface with a 1-km resolution (from 30 N latitude to the North Pole) [30]. The achieved vertical accuracy was around 230 m.

Finally, the Magellan spacecraft [31] was launched by NASA in 1989. The radar on-board [32] collected SAR images, combined with altimetry and radiometry measurements at a frequency of 2.3 GHz, over the majority of Venus' surface. The resolution of the SAR images was better than 150 m over more than half the planet. The vertical accuracy of the altimeter was better than 50 m. Combining all the information available, a map of the elevation was built for the whole planet (see Fig. 2, center). The SAR of the Magellan spacecraft also provided very detailed images [33] (see Fig. 2, right) of volcanic

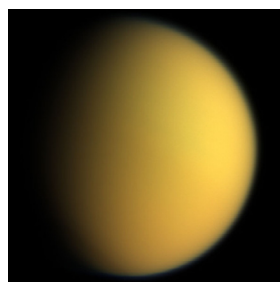


Image credit : NASA/JPL/Space Science Institute public PIA06230

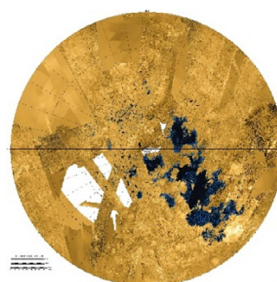


Image credit: NASA/JPL-Caltech

Fig. 3. Images of Titan: Left: Color composite image of Titan taken during the *Cassini* spacecraft's flyby in 2005 [PIA06230]. A thick orange haze prevents any view of the surface. Right: Colorized mosaic of Titan's northern land of lakes and seas obtained by the multimode radar [34]. The dry areas are displayed in brown, and the areas interpreted as liquid hydrocarbon bodies in blue (PIA17655).

and tectonic structures that revealed that Venus' geology is dominated by volcanism. The impact craters that were detected too appeared to be evenly spread over the Venusian surface, which implies that the planet's entire surface is the same age. Crater counting suggests an age of 1 billion years.

3.1.2. Titan

The *Cassini* NASA mission was launched in 2005 to explore Saturn, its rings and satellites. A special attention was paid to Titan, which is the only moon in the Solar System with a thick atmosphere (10 times thicker than the Earth's one) that prevents observation of its surface at optical wavelengths (see Fig. 3, left). The Huygens ESA probe successfully landed on its surface while the main spacecraft remained in orbit around Saturn. Impressive sets of radar data have been collected during more than one hundred flybys of Titan. The radar on-board the orbiter [25] is a powerful multimode system that can operate as a SAR, radar altimeter, scatterometer and radiometer. Its principal objective is to characterize the surface of Titan on a regional scale. The obtained SAR images, whose resolution is > 350 m, have shown the existence, mostly in the northern hemisphere, of flat and smooth areas, which have been interpreted as lakes and seas of ethane and methane (see Fig. 3, right) [34]. Overlapping SAR images have been used locally to build SAR digital elevation models by radar stereogrammetry [35]. The achieved resolution is of several kilometers horizontally and around 100 m vertically, which is significantly better than the altimeter's capacity.

The radar observations also revealed the presence of numerous impact craters, of dunes whose size and pattern vary with altitude and latitude [36], of river channels [37], of mountains [38], of sedimentary basins [39], and karstic landscapes [40].

3.2. Sounding beneath the surface

Unlike Titan and Venus's surface, the surface of Mars, Mercury and the Moon are readily accessible to optical remote sensing from orbit, but radar operated at low-enough frequency have the unique capacity to sound through the surface and access the buried structures.

3.2.1. The subsurface of Mars

So far Mars has been the object of a number of missions that are more and more interested in discovering what is beneath its surface. The rare clouds present in the Martian atmosphere do not prevent optical remote sensing of the surface from orbit and large datasets obtained by spectro-imagers and context and high-resolution stereoscopic cameras are now available. Till now, two orbital radars have been designed and used to retrieve information about the Martian subsurface. The MARSIS orbital radar sounder, onboard ESA's Mars Express spacecraft launched in 2003, was designed to investigate the Martian ionosphere and the geological and hydrological structure of the subsurface, with a particular emphasis on the detection of deep bodies of solid or liquid water [41]. MARSIS operates at frequencies of ~ 2 –5 MHz; its horizontal resolution is about 10 km while the range accuracy is 150 m in vacuum [42]. The particularly low frequencies used by the instrument give it a theoretical ability to detect the presence of liquid water, under ideal sounding conditions, at depths of up to ~ 3 –5 km beneath the Martian surface [43]. In practice, MARSIS has achieved this level of sounding performance only in a number of specific environments, which include the ice-rich (and, thus, low dielectric loss) North and South Polar Caps (see Fig. 4 [44]), where it provided estimates of the thickness of ice deposits, as well as several other sites at lower latitudes. Of the latter, the most notable is the Medusae Fossae Formation, whose radar propagation characteristics are consistent with a composition ranging from a dry, highly porous pyroclastic deposit at one extreme to an ice-rich sedimentary deposit at the other, potentially formed by the redistribution of polar volatiles at times of high obliquity [45]. Hints of several other moderately deep reflectors have also been found in the vicinity of Ma'adim Vallis, where there is evidence that they may originate from lithological interfaces [46].

MARSIS was closely followed by the flight of another radar sounder called the SHallow RADar (SHARAD) on the Mars Reconnaissance Orbiter (MRO) [47]. SHARAD was designed to complement the capabilities and performance of MARSIS

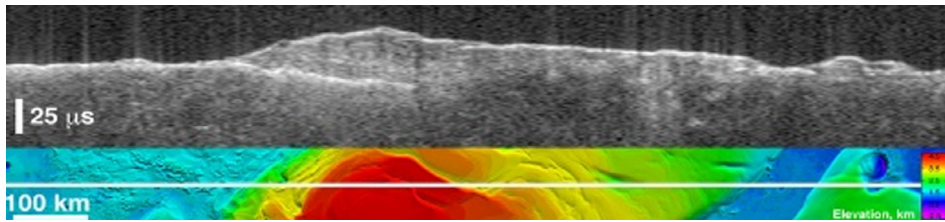


Image Credit : NASA / JPL / ASI / ESA / Univ. of Rome / MOLA Science Team [43]

Fig. 4. Top: MARSIS radargram of the South Pole area. Bottom: The white line on the image shows the corresponding ground track shown on a topographic map of the area based on data from the MOLA laser altimeter on board NASA's Mars Global Surveyor.

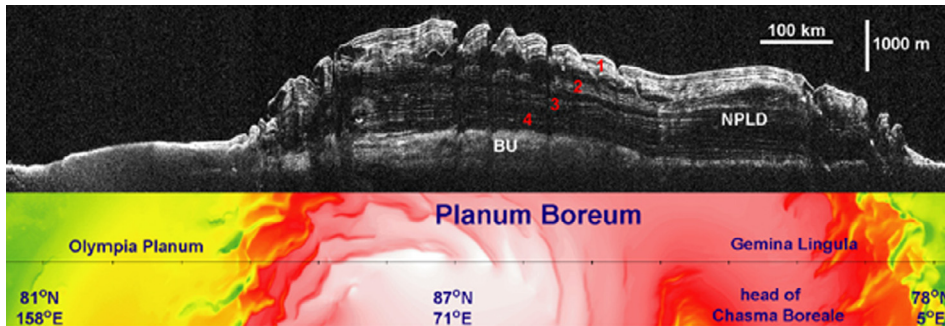


Image Credit: NASA/JPL-Caltech/University of Rome/SwR

Fig. 5. Top: SHARAD radargram of the North Polar Layered Deposits (NPLD) over the Basal Unit (BU). Bottom: MOLA laser topography along the ground track [47].

by operating at higher frequencies around 20 MHz to better resolve variations in near-surface composition, stratigraphy and structure – particularly with regard to resolving the internal layers of the polar caps (see Fig. 5 [48]). The horizontal resolution of the instrument is between 0.3 and 3 km and the vertical resolution is about 15 m (10 times better than MARSIS). Comparison of Figs. 4 and 5 gives a clear understanding of the better resolution that can be obtained at higher frequencies because of the associated increase in the frequency bandwidth.

Outside the polar caps, ShaRad soundings performed in the eastern Hellas region revealed electromagnetic properties that are consistent with massive water ice, supporting the hypothesis that ground ice is present in the subsurface at lower latitudes [49].

The future ESA/Roscosmos ExoMars rover Mission [12] to Mars, which is currently planned for 2018, will have onboard a ground penetrating radar designed to sound the very shallow subsurface (to a depth of ~ 3 m) along the rover path. This radar called WISDOM [50] (Water Ice Subsurface Deposits Observation on Mars) has been designed to provide a range resolution better than 10 cm in the subsurface and is thus operating over a large-frequency bandwidth between 0.5 and 3 GHz. It will provide information about the geological context and help to the identification of potentially habitable sites. The drill of the mission will then collect, at a depth < 2 m, samples that will be analyzed by a suite of instruments onboard the rover. WISDOM is a step frequency radar, thus it transmits a number of continuous wave signals, each at a single frequency rather than a single pulse. A complete set of measurements is performed for the range of frequencies covered by the instrument's bandwidth. Performing an Inverse Fourier Transform on the whole set of frequency responses allows the computation of the impulse response, which would be readily obtained by a pulse GPR. This step frequency technique allows a better use of the limited power available on the rover. In addition, the antenna system has been designed to allow polarimetric measurements, which will provide additional information about the shape and orientation of the reflecting structures. Given the mission's constraints, WISDOM will be accommodated on the rover at a distance of about 30 cm from the surface, which is unusual for a GPR whose antennas are usually in contact with the ground. This specific configuration is not the most favorable, but provides the opportunity to make use of the surface echo to get an estimate of the top layer dielectric constant. A prototype of the instrument very similar to the final flight model (with a total mass of 1.7 kg) is currently tested in various environments. Fig. 6 illustrates the ability of the instrument to resolve fine layering thanks to its broad frequency bandwidth [51]. A radargram obtained with only 1 GHz of frequency bandwidth is presented for comparison.

The next Mars2020 NASA mission has also selected a GPR operating at slightly lower frequencies to be part of its payload [52]. This GPR called RIMFAX (Radar Imager for Mars' Subsurface Exploration) is currently under development. RIMFAX is a gated Frequency Modulated Continuous Wave (FMCW) radar operating over the frequency band 150–1200 MHz, which should allow it to probe the Martian subsurface to depths > 10 m.

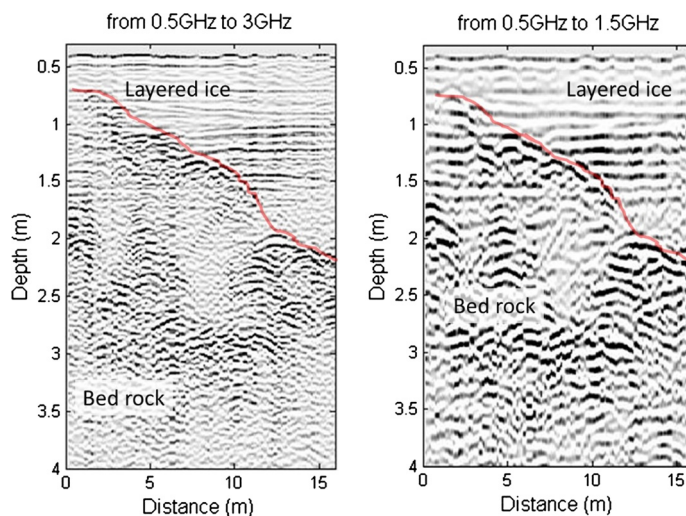


Fig. 6. Examples of radargrams obtained by WISDOM in the Dachstein ice cave [51], Austria (with the whole frequency bandwidth on the left and with only 1 GHz of bandwidth on the right). The layered ice is visible on the upper right part of the figures. The red line highlights the transition with the bedrock beneath the ice.

3.2.2. The subsurface of the Moon

Even if the Martian polar caps provided so far the best examples of planetary features explored by radar, the Moon was also sounded by radars. The NASA Explorer 35 bistatic experiment [53] was launched in 1967; its purpose was to study the electromagnetic reflective properties of the lunar surface. The experiment used the 136.10-MHz communication channel between the spacecraft and the Earth, the electromagnetic waves were scattered from the lunar surface and then recorded at Stanford on Earth. Statistics of the lunar surface's slope were obtained in the equatorial region.

The first successful attempt to sound the lunar subsurface from orbit was performed in 1972 during the Apollo 17 mission (ALSE experiment [54]). The measurements performed at 5 and 150 MHz allowed the detection of a layer at kilometeric depths in two sounded lunar maria and validated the feasibility of such measurements [55]. In 2007, the LRS (Lunar Radar Sounding) instrument on-board the Kaguya spacecraft of the JAXA SELENE mission completed a global coverage of the lunar surface and subsurface at 5 MHz [56]. Subsurface features observed by both ALSE and LRS radars are interpreted as interfaces between lava flows of different ages.

Two mini-SAR (or mini-RF) have been designed and used to explore the Moon [57,58]. The first instrument was launched on the Indian Space Research Organization's (ISRO's) Chandrayaan-1 spacecraft, while the second one was on-board the NASA's Lunar Reconnaissance Orbiter (LRO). They have mapped both polar regions and a number of different geologic units on the lunar surface. Mini SAR instruments have been designed to map the permanently dark areas of the lunar polar regions to search for potential water ice deposits. The search for water ice is their primary science objective, but they also characterized the surface roughness and thickness of the regolith. The Mini SAR transmits Right Circular Polarization at 2.5 GHz and receives both Left and Right, which gives access to the circular polarization ratio. The elevated CPR (Circular Polarization Ratio) values observed within permanently shadowed craters in the polar areas are consistent with the presence of water ice in these craters [59].

3.2.3. The nucleus of comet Churyumov–Gerasimenko

Despite numerous observations of comets either from Earth or during dedicated space missions among which ESA's Giotto, NASA's Deep Space, Stardust and Deep Impact [60], there has been, prior to the *Rosetta* mission, no direct access to the structure of cometary nuclei. The successful *Rosetta* mission [61] with the recent descent and landing of *Philae* on the nucleus of 67P/Churyumov–Gerasimenko at the end of 2014 has provided for the first time in-situ data of the upper most importance. With receivers and transmitters onboard both *Rosetta* and *Philae*, the objective of the CONSERT (Comet Nucleus Sounding Experiment by Radiowave Transmission) radar is the characterization of the nucleus in terms of internal structure and dielectric properties. CONSERT [62] is a bi-static radar that consists of two separate units: The Lander CONSERT unit (LCN) located on *Philae* and the Orbiter CONSERT unit (OCN) located on the orbiter. A radio signal at 90 MHz is transmitted by the OCN and propagates through the comet nucleus to the LCN. The LCN works as a transponder: the signal received by the lander is analyzed in real time to detect the strongest echo (which is expected to be the first one) for synchronization purposes, and immediately retransmitted back to the orbiter, where the final data is eventually recorded. The propagation delay and amplitude of the received echoes measured are readily obtained from the measured impulse response. For each sounding configuration, the measured propagation delay corresponding to the first echo allows one to estimate the average dielectric constant of the nucleus along the propagation path, and to constrain the composition and porosity of the nucleus. The width of the received echoes is an indirect measurement of the internal heterogeneity at a scale larger than the experiment wave length (~ 3 m), while the measured amplitude can be linked to attenuation

and/or diffusion inside the nucleus. Despite the significant polarization mismatch between lander and orbiter's antennas due to the fact that *Philae* is not standing on its three feet, some good-quality data have been obtained. They show that the waves did propagate through the smaller lobe of the nucleus. The measured delays provided an estimate of the averaged dielectric constant value of about 1.27, which suggests a porosity larger than 78% [63]. The analysis of the data also shows that scattering inside the nucleus is very limited [63], which suggests that the nucleus is rather homogeneous at scales of the order of magnitude of the wavelength and that the permittivity at depth is probably lower inside the nucleus than at the surface [64]. CONSERT measurements have even been able to provide an estimate of the *Philae* location inside a strip of 350×30 m at the surface [65] but, to actually quantitatively characterize the nucleus internal structure, an accurate knowledge of the experiment geometry (Orbiter and Lander location and attitude with respect to a 3D nucleus shape model) is needed. Whenever the actual location and position of *Philae* can be better constrained, the thorough analysis and interpretation of the data collected by CONSERT that takes into account the amplitude of the received signals will be possible.

An updated version of this tomographic radar concept is currently considered for the future Asteroid Impact Mission (AIM) aiming at asteroid Dydimos characterization [66].

3.2.4. Icy moons of Jupiter

The three Jupiter icy moons (Ganymede, Europa and Callisto) are believed to hide liquid-water oceans beneath a several-km-thick crust of ice. Detection and characterization of these oceans would be essential to support the potential habitability of these moons and to make significant progress on our understanding of the life. Since electromagnetic waves experience little attenuation in ice (see § 2.2.1. the deep soundings of the Martian polar caps) and would be strongly reflected by large bodies of liquid water, radars are particularly well suited to this objective. Consequently, the future missions aiming to Jupiter and its icy moons will carry onboard radars designed to perform deep sounding of the ice crust.

The frequency of the electromagnetic waves used has to be carefully chosen: on one side, it should be as low as possible to maximize the penetration capability and to minimize the scattering at the surface due to roughness. On the other side, the intense natural Jovian radio emissions at frequencies below 40 MHz [67] need to be taken into account when planning the radar operations and the size of the antenna, which is commensurate with the wavelength, must be kept within reasonable dimensions.

The Jupiter Icy Moon Explorer (JUICE) ESA mission [68] will be launched in 2022 to study Jupiter and investigate the potential habitability of its icy moons. Among the payload instruments, the radar sounder called RIME (Radar for Icy Moon Exploration) [69] has been designed to study the subsurface structure of the moons up to depths about 9 km in ice. A center frequency of 9 MHz has been chosen to achieve this objective. The high-resolution mode with a 3-MHz bandwidth will allow the instrument to achieve a vertical resolution of 30 m in the ice. A lower resolution mode is also planned with a 1-MHz bandwidth to reduce the data volume. The use of the 9-MHz center frequency will restrain the radar operation to the side of Europa which is away from Jupiter.

Among Jupiter's icy moons, Europa is currently considered to be the most promising location in the Solar System to search for signs of extant life. The future NASA Europa mission, formerly known as Europa Clipper, [70] should be launched in the mid-2020s and perform 45 flybys of Europa at altitudes varying from 2700 to 25 kilometers above the surface. The Radar for Europa Assessment and Sounding: Ocean to Near-surface (REASON) [71] instrument has been selected for the mission. As mention previously, the choice of the frequency is crucial, REASON will use two frequencies: a shorter 60-MHz wave (which is not jammed by the radio emission of Jupiter) and a longer 9-MHz wave (which will ensure deep penetration but will be operated only on the anti-Jovian side of Europa). This dual-frequency radar is designed to look for a potential liquid water reservoir, but also to characterize the structures of the ice shell. The possibility to complement the orbiter with a lander that might have a stationary radar on-board is currently under study.

4. Conclusion

This brief overview demonstrates the essential contribution of radars to the exploration of the Solar System.

Radars can be highly adapted to different scientific objectives and platforms. Most of the future space missions will have among their payload radars that have been specifically designed to provide information essential to the understanding of studied bodies' formation and evolution.

From the surface, each of the next rover missions to Mars (ExoMars and Mars2020) will accommodate a Ground Penetrating Radar to discover along the rover path the geologic features buried under the Martian subsurface. GPRs might soon become mandatory instruments on a rover payload just like cameras are at the moment. The synergy between these two context instruments is obvious [72], and will give the possibility to have a better understanding of the site's geological histories and, for example, to assess their capacity to have been habitable in the past.

From orbit, some of the most spectacular features revealed by sounding radars have been obtained by the *Cassini* radar on Titan and the MARSIS and ShaRad sounders on the Martian polar caps. Jupiter's icy moons, with their potential hidden oceans, are future challenges in the exploration of the Solar System, and radars will provide data that will allow us to make significant progress in our understanding of the Solar System formation and evolution.

Finally, some quite specific tomographic radars like the CONSERT radar of the *Rosetta* mission are designed to sound small bodies of the Solar System (comets, asteroids). The AIM (Asteroid Impact Mission) ESA mission, currently under phase

B study, is aiming at the 65803 Didymos binary asteroid system. The scenario is to land on the asteroid's moon a small lander that would allow an updated version of the CONSERT radar to be operated in order to characterize the interior of the moon.

References

- [1] D. Fink, The radar equation, *Electronics* 18 (1945) 92–94.
- [2] J. Mofensen, Radar echoes from the moon, *Electronics* 19 (1946) 92–98.
- [3] Z. Bay, Reflection of microwaves from the moon, *Hung. Acta Phys.* 1 (1946) 1–22.
- [4] D.O. Muhleman, D.B. Holdridge, N. Block, Determination of the astronomical unit from velocity, range, and integrated velocity data, and the Venus–Earth ephemeris, in: W.K. Victor, R. Stevens, S.W. Golomb (Eds.), *Radar Exploration of Venus: Goldstone Observatory Report for March–May 1961*, pp. 83–92, Technical report 32-132.
- [5] M.A. Slade, L.A.M. Benner, A. Silva, Goldstone Solar System radar observatory: Earth-based planetary mission support and unique science results, *Proc. IEEE* 99 (5) (2011) 757–769, <http://dx.doi.org/10.1109/JPROC.2010.2081650>.
- [6] R.B. Dyce, G.H. Pettengill, I.I. Shapiro, Radar determination of the rotations of Venus and Mercury, *Astron. J.* 72 (3) (1967) 351–359, <http://dx.doi.org/10.1086/110231>.
- [7] A.F. Chicarro, Science Team, The Mars Express mission and its Beagle-2 lander, in: *Sixth International Conference on Mars, 20–25 July 2003, Pasadena, CA, USA*, abstract No. 3049.
- [8] M.D.D. Johnston, J.E. Graf, R.W. Zurek, H.J. Eisen, B. Jai, The Mars Reconnaissance Orbiter mission, in: *2005 IEEE Aerospace Conference, 5–12 March 2005*, pp. 447–464, <http://dx.doi.org/10.1109/AERO.2005.1559336>.
- [9] R.S. Saunders, et al., Magellan mission summary, *J. Geophys. Res.* 97 (E8) (1992) 13067–13090, <http://dx.doi.org/10.1029/92JE01397>.
- [10] D.L. Matson, et al., The *Cassini/Huygens* mission to the Saturnian System, *Space Sci. Rev.* 104 (1–4) (2002) 1–58, <http://dx.doi.org/10.1023/A:1023609211620>.
- [11] Y. Su, et al., Data processing and initial results of Chang'e-3 lunar penetrating radar, *RAA* 14 (12) (2014) 1623–1632, <http://dx.doi.org/10.1088/1674-4527/14/12/010>.
- [12] J.L. Vago, G. Kminek, Putting together an exobiology mission: the ExoMars example, in: G. Horneck, P. Rettberg (Eds.), *Complete Course in Astrobiology, Wiley-VCH Verlag GmbH & Co. KGaA, Weinheim, Germany, 2007*.
- [13] W. Kofman, et al., Comet nucleus sounding experiment by radiowave transmission, *Adv. Space Res.* 21 (11) (1998) 1589–1598.
- [14] M. Biancheri-Astier, R. Hassen-Khodja, V. Ciarletti, C. Corbel, Y. Simon, C. Caudoux, J. Faroux, F. Dolon, EISS: an HF mono and bistatic GPR for terrestrial and planetary deep sounding, Lecce, Italy, 2010, GPR2010.
- [15] A. Le Gall, V. Ciarletti, J.J. Berthelier, A. Reineix, C. Guiffaut, R. Ney, F. Dolon, S. Bonaimé, R. Clairquin, D. Nevejans, An imaging HF GPR using stationary antennas: experimental validation over the Antarctic ice sheet, *IEEE Trans. Geosci. Remote Sens.* 46 (12) (2008) 3975–3986, <http://dx.doi.org/10.1109/TGRS.2008.2000718>.
- [16] V. Ciarletti, A. Le Gall, S.M. Clifford, Ch. Corbel, F. Dolon, R. Ney, J.J. Berthelier, Bistatic sounding of the deep subsurface with a ground penetrating radar – experimental validation, *Planet. Space Sci.* 117 (2015) 177–183, <http://dx.doi.org/10.1016/j.pss.2015.06.008>.
- [17] R.A. Simpson, et al., Polarization in bistatic radar probing of planetary surfaces: application to Mars express data, *Proc. IEEE* 99 (5) (2011), <http://dx.doi.org/10.1109/JPROC.2011.2106190>.
- [18] S. Nozette, et al., The Clementine bistatic radar experiment, *Science* 274 (5292) (1996) 1495–1498.
- [19] R.A. Simpson, G.L. Tyler, J.P. Brenkle, M. Sue, Viking bistatic radar observations of the Hellas basin on Mars: preliminary results, *Science* 203 (1979) 45–46.
- [20] L.J. Porcello, et al., The Apollo Lunar sounder radar system, *Proc. IEEE* 62 (6) (1974) 769–783.
- [21] G. Picardi, et al., Radar soundings of the subsurface of Mars', *Science* 310 (23 Dec. 2005) 1925–1929.
- [22] Roger J. Phillips, et al., Mars north polar deposits: stratigraphy, age, and geodynamical response, *Science* 320 (2008) 1182, <http://dx.doi.org/10.1126/science.1157546>.
- [23] Takayuki Ono, Hiroshi Oya, Lunar radar sounder (LRS) experiment on-board the SELENE spacecraft, *Earth Planets Space* 52 (2000) 629–637.
- [24] Yu.N. Aleksandrov, et al., A planet rediscovered: results of Venus radar imaging from the Venera 15 and Venera 16 spacecraft, *Sov. Sci. Rev., E, Astrophys. Space Phys.* 6 (1) (Aug. 1988) 61–101.
- [25] W.T.K. Johnson, Magellan imaging radar mission to Venus, *Proc. IEEE* 79 (6) (1991) 777–790, <http://dx.doi.org/10.1109/5.90157>.
- [26] C. Elachi, M.D. Allison, L. Borgarelli, P. Encrenaz, E. Im, M.A. Janssen, W.T.K. Johnson, R.L. Kirk, R.D. Lorenz, J.I. Lunine, D.O. Muhleman, S.J. Ostro, G. Picardi, F. Posa, C.G. Rapley, L.E. Roth, R. Seu, L.A. Soderblom, S. Vetrilla, S.D. Wall, C.A. Wood, H.A. Zebker, RADAR: the *Cassini* Titan radar mapper, *Space Sci. Rev.* 115 (2004) 71–110.
- [27] W.B. Rossow, A.D. Del Genio, S.S. Limaye, L.D. Travis, Cloud morphology and motions from Pioneer Venus images, *J. Geophys. Res.* 85 (1980) 8107–8128.
- [28] G.H. Pettengill, et al., Pioneer Venus radar mapper experiment, *Science* 203 (4382) (1979) 806–808.
- [29] G.H. Pettengill, E. Eliason, P.G. Ford, G.B. Loriot, H. Masursky, G.E. McGill, Pioneer Venus Radar results altimetry and surface properties, *J. Geophys. Res.* 85 (A13) (1980) 8261–8270, <http://dx.doi.org/10.1029/JA085iA13p08261>.
- [30] V.L. Barsukov, et al., The geology and geomorphology of the Venus surface as revealed by the radar images obtained by Veneras 15 and 16, in: *Proc. of the Sixteenth Lunar and Planetary Science Conference, J. Geophys. Res.* 91 (B4) (1986) D378–D398, Part 2.
- [31] S.S. Dallas, N.L. Nickle, The Magellan mission to Venus. Advances in astronomical sciences. Part 1, *Aerosp. Cent.* 21 (64) (1987), AAS 86–331.
- [32] J.P. Ford, R.G. Blom, J.A. Crisp, C. Elachi, T.G. Farr, R.S. Saunders, E.E. Theilig, S.D. Wall, S.B. Yewell, *Spaceborne Radar Observations: A Guide for Magellan Radar Image Analysis*, JPL Pub., 1989, 89–41, 126 p.
- [33] R.S. Saunders, G.H. Pettengill, R.E. Arvidson, B. Sjogren, W.T.K. Johnson, L.J. Pieri, The Magellan Venus radar mapping mission, *J. Geophys. Res.* 95 (B6) (1990) 8339–8355.
- [34] Stofan, et al., The lakes of Titan, *Nature* 445 (2007) 61–64, <http://dx.doi.org/10.1038/nature05438>.
- [35] M.C. Lopes, et al., Cryovolcanism on Titan: new results from *Cassini* RADAR and VIMS, *J. Geophys. Res., Planets* 118 (2013) 1–20, <http://dx.doi.org/10.1029/2012JE004239>.
- [36] A. Le Gall, M.A. Janssen, L.C. Wye, A.G. Hayes, J. Radebaugh, C. Savage, H. Zebker, R.D. Lorenz, J.I. Lunine, R.L. Kirk, R.M.C. Lopes, S. Wall, P. Callahan, E.R. Stofan, T. Farr, The *Cassini* Radar Team, SAR, radiometry, scatterometry and altimetry observations of Titan's dune fields, *Icarus* 213 (2011) 608–624.
- [37] A. Le Gall, M.A. Janssen, P. Paillou, R.D. Lorenz, S.D. Wall, Radar-bright channels on Titan, *Icarus* (ISSN 0019-1035) 207 (2) (2010) 948–958, <http://dx.doi.org/10.1016/j.icarus.2009.12.027>.
- [38] J. Radebaugh, R.D. Lorenz, R.L. Kirk, J.I. Lunine, E.R. Stofan, R.M.C. Lopes, S.D. Wall, Mountains on Titan observed by *Cassini* Radar, *Icarus* 192 (1) (2007) 77–91.
- [39] T. Cornet, O. Bourgeois, S. Le Mouélis, S. Rodriguez, T. Lopez Gonzalez, C. Sotin, G. Tobie, C. Fleurant, J.W. Barnes, R.H. Brown, K.H. Baines, B.J. Buratti, R.N. Clark, P.D. Nicholson, Geomorphological significance of Ontario Lacus on Titan: integrated interpretation of *Cassini* VIMS, ISS and RADAR data and comparison with the Etosha Pan (Namibia), *Icarus* 218 (2012) 788–806.

- [40] T. Cornet, D. Cordier, T.L. Bahers, O. Bourgeois, C. Fleurant, S.L. Mouélic, N. Altobelli, Dissolution on Titan and on Earth: toward the age of Titan's karstic landscapes, *J. Geophys. Res.*, Planets 120 (2015) 1044–1074, <http://dx.doi.org/10.1002/2014JE004738>.
- [41] Giovanni Picardi, et al., Radar soundings of the subsurface of Mars, *Science* 310 (5756) (2005) 1925–1928, <http://dx.doi.org/10.1126/science.1122165>.
- [42] G. Picardi, et al., Performance and surface scattering models for the Mars advanced radar for subsurface and ionosphere sounding (MARSIS), *Planet. Space Sci.* 52 (2004) 149–156.
- [43] R. Orosei, et al., Mars advanced radar for subsurface and ionospheric sounding (MARSIS) after nine years of operation: a summary, *Planet. Space Sci.* 112 (2014) 3785 98–114, <http://dx.doi.org/10.1016/j.pss.2014.07.010>.
- [44] J.J. Plaut, G. Picardi, et al., Subsurface radar sounding of the South polar layered deposits of Mars, *Science* 316 (5821) (2007) 92–95.
- [45] T.R. Watters, et al., Radar sounding of the Medusae Fossae Formation Mars: equatorial ice or dry, low-density deposits?, *Science* 318 (5853) (2007) 1125, <http://dx.doi.org/10.1126/science.1148112>.
- [46] O. White, et al., MARSIS radar sounder observations in the vicinity of Ma'adim Vallis, Mars, *Icarus* 201 (2009) 460, <http://dx.doi.org/10.1016/j.icarus.2009.01.015>.
- [47] R. Seu, et al., SHARAD sounding radar on the Mars Reconnaissance Orbiter, *J. Geophys. Res.* 112 (2007) E05S05, <http://dx.doi.org/10.1029/2006JE002745>.
- [48] Nathaniel E. Putzig, Roger J. Phillips, Bruce A. Campbell, John W. Holt, Jeffrey J. Plaut, Lynn M. Carter, Anthony F. Egan, Fabrizio Bernardini, Ali Safaeinili, Roberto Seu, Subsurface structure of planum Boreum from Mars Reconnaissance Orbiter Shallow Radar soundings, *Icarus* 204 (2) (2009) 443–457.
- [49] J. Plaut Jeffrey, A. Safaeinili, J.W. Holt, R.J. Phillips, J.W. Head III, R. Seu, N.E. Putzig, A. Frigeri, Radar evidence for ice in lobate debris aprons in the mid-northern latitudes of Mars, *Geophys. Res. Lett.* 36 (2009) L02203, <http://dx.doi.org/10.1029/2008GL036379>.
- [50] V. Ciarletti, C. Corbel, D. Plettemeier, P. Cais, S.M. Clifford, S.E. Hamran, WISDOM a GPR designed for shallow and high resolution sounding of the Martian subsurface, *Proc. IEEE* 99 (5) (2011) 824–836, <http://dx.doi.org/10.1109/JPROC.2010.2100790>.
- [51] S. Dorizon, V. Ciarletti, D. Plettemeier, W.-S. Benedix, Performance validation of the ExoMars 2018 WISDOM GPR in ice caves, Austria, *Planet. Space Sci.* 120 (2016) 1–14.
- [52] S.E. Hamran, H.E.F. Amundsen, L.M. Carter, R.R. Ghent, J. Kohler, M.T. Mellon, D.A. Paige, The RIMFAX ground penetrating radar on the Mars 2020 Rover, American Geophysical Union, Fall Meeting 2014, abstract #P11A-3746.
- [53] G.L. Tyler, R.A. Simpson, Bistatic radar measurements of topographic variations in lunar surface slopes with explorer 35, *Radio Sci.* 5 (2) (1970) 263–271, <http://dx.doi.org/10.1029/RS005i002p00263>.
- [54] L.J. Porcello, R.L. Jordan, J.S. Zelenka, G.F. Adams, R.J. Phillips, W.E. Brown Jr., S.H. Ward, P.L. Jackson, The Apollo lunar sounder radar system, *Proc. IEEE* 62 (1974) 769–783.
- [55] W.J. Peeples, W.R. Sill, T.W. May, S.H. Ward, R.J. Phillips, R.L. Jordan, E.A. Abbott, T.J. Killpack, Orbital radar evidence for lunar subsurface layering in Maria Serenitatis and Crisium, *J. Geophys. Res.* 83 (1978), <http://dx.doi.org/10.1029/JB083iB07p03459>.
- [56] A. Pommerol, W. Kofman, J. Audouard, C. Grima, P. Beck, J. Mouginot, A. Hérique, A. Kumamoto, T. Kobayashi, T. Ono, Detectability of subsurface interfaces in lunar maria by the LRS/SELENE sounding radar: influence of mineralogical composition, *Geophys. Res. Lett.* 37 (2010) L03201, <http://dx.doi.org/10.1029/2009GL041681>.
- [57] P.D. Spudis, et al., Mini-SAR: an imaging radar experiment for the Chandrayaan-1 mission to the Moon, *Curr. Sci.* 96 (4) (2009).
- [58] D.B.J. Bussey, P.D. Spudis, the Mini-RF Team, New insights into lunar processes and history from global mapping by Mini-RF radar, *Lunar Planet. Sci.* 42 (2011) 2086.
- [59] P.D. Spudis, et al., Evidence for water ice on the moon: results for anomalous polar craters from the LRO Mini-RF imaging radar, *J. Geophys. Res., Planets* 118 (2013), <http://dx.doi.org/10.1002/jgre.20156>.
- [60] M.A. Barucci, E. Dotto, Anny Chantal Levasseur-Regourd, Space missions to small bodies: asteroids and cometary nuclei, *Astron. Astrophys. Rev.* 19 (1) (2011) 48 (29 p).
- [61] Luigi Colangeli, Elena Mazotta Epifani, Pasquale Palumbo, *The New Rosetta Targets: Observations, Simulations, and Instrument Performances*, Springer-Verlag, New York, 2004, 315 p.
- [62] Kofman, et al., The comet nucleus sounding experiment by radiowave transmission (CONSERT): a short description of the instrument and of the commissioning stages, *Space Sci. Rev.* 128 (2007) 413–432.
- [63] <http://blogs.esa.int/rosetta/2014/11/21/homing-in-on-philae-final-landing-site/>.
- [64] Kofman, et al., Preliminary results from CONSERT experiment on Rosetta mission, AGU 2014, P34B-01, San Francisco, CA, USA, 2014.
- [65] V. Ciarletti, A.C. Levasseur-Regourd, J. Lasue, C. Statz, D. Plettemeier, A. Hérique, Y. Rogez, W. Kofman, CONSERT suggests a change in local properties of 67P/Churyumov–Gerasimenko's nucleus at depth, *Astron. Astrophys.* 583 (2015) A40, <http://dx.doi.org/10.1051/0004-6361/201526337>.
- [66] P. Michel, et al., Science case for the asteroid impact mission (AIM): a component of the Asteroid Impact & Deflection Assessment (AIDA) mission, *Adv. Space Res.* 57 (12) (2016) 2529–2547, <http://dx.doi.org/10.1016/j.asr.2016.03.031>.
- [67] L. Bruzzone, G. Alberti, C. Catallo, A. Ferro, W. Kofman, R. Orosei, Subsurface radar sounding of the Jovian moon Ganymede, *Proc. IEEE* 99 (5) (2011).
- [68] O. Grasset, et al., Jupiter icy moons explorer (JUICE): AN ESA mission to orbit Ganymede and to characterize the Jupiter system, *Planet. Space Sci.* 78 (2013) 1–21.
- [69] L. Bruzzone, et al., RIME: radar for icy Moon exploration, EPSC Abstr. 8 (2013), EPSC2013-744-1.
- [70] C.B. Phillips, R.T. Pappalardo, Europa clipper mission concept: exploring Jupiter's ocean moon, *Eos* 95 (20) (2014).
- [71] A. Mousessian, D.D. Blankenship, J. Plaut, G.W. Patterson, Y. Gim, D.M. Schroeder, K.M. Soderlund, D. Young, C. Grima, E. Chapin, REASON for Europa, AGU Fall Meeting, San Francisco, 2015.
- [72] G. Paar, G. Hesina, C. Traxler, V. Ciarletti, D. Plettemeier, C. Statz, K. Sander, B. Nauschnegg, Embedding sensor visualization in Martian terrain reconstructions, in: Proceedings of ASTRA, 2015.